



International Institute for
Applied Systems Analysis
Schlossplatz 1
A-2361 Laxenburg, Austria

Tel: +43 2236 807 342
Fax: +43 2236 71313
E-mail: publications@iiasa.ac.at
Web: www.iiasa.ac.at

Interim Report

IR-09-066

A derivation of the statistical characteristics of forest fires

Jianyi Lin (jianyi.lin@unimi.it)

Sergio Rinaldi (rinaldi@elet.polimi.it)

Approved by

Ulf Dieckmann
Leader, Evolution and Ecology Program

June 2010

Interim Reports on work of the International Institute for Applied Systems Analysis receive only limited review. Views or opinions expressed herein do not necessarily represent those of the Institute, its National Member Organizations, or other organizations supporting the work.

26 **Empirical evidence of forest fires characteristics**

27 Forest fires have been observed for centuries all over the world, and huge
28 data sets are now of public domain. They usually contain long series of
29 fire events identified by location, time of occurrence, and burned area.
30 Statistical analyses of these data sets have allowed various authors to
31 identify, on a purely empirical basis, general characteristics of forest
32 fires.

33 Malamud et al. (1998) and Ricotta et al. (1999) were the first to
34 perform statistics of the burned areas. They arrived to the same con-
35 clusion, namely that burned areas are distributed as a power law, rep-
36 resented by a straight line in log-log scale. This conclusion is actually
37 surprising, because the only graph reported in Ricotta et al. (1999)
38 clearly shows that the distributions of small, medium and large fires
39 are well approximated by different power laws, and the same, though
40 less pronounced, effect is detectable in the plots obtained by Malamud
41 et al. (1998). Most likely, this slightly distorted interpretation of the
42 results had two targets: find an agreement with the theoretical studies
43 available at that time on self-organized critical forest-fire models (see
44 next section), and support the idea that the knowledge of the occur-
45 rence frequency of small and medium fires can be used to quantify the
46 risk of large fires.

47 [Figure 1 about here.]

48 Subsequent studies (Ricotta et al. (2001); Song et al. (2001); Reed
49 and McKelvey (2002) and, in particular, Ricotta (2003)) confirmed that
50 the distributions of the burned areas are smooth but can sometimes be
51 approximated by three or two different power laws, as shown in Fig. 1,
52 where three examples taken from the literature are reported.

53 A few years later, the first studies on the temporal distributions
54 of the fire events are performed through various statistical techniques
55 (Telesca et al. (2005); Lasaponara et al. (2005); Ricotta et al. (2006)).

56 The main result is the discovery of a high degree of time-clusterization
 57 even if the burned areas are not distributed as a power-law. This means
 58 that the occurrence of large events mimics the process of occurrence of
 59 smaller events, thus allowing one to model the scarce big fires on the
 60 basis of the abundant small fires. This is neatly pointed out in Corral
 61 et al. (2008) where the fire catalog for all Italy in the period 1998-
 62 2002 is used to estimate the probability density $D(\tau|s)$ of the time
 63 intervals τ separating two successive fires within the so-called class-
 64 s fires (i.e., fires with burned areas greater than or equal to s). The
 65 distributions estimated for each class (see the curves displayed in Fig.
 66 2(a) reproduced from Corral et al. (2008)) can somehow be fitted with
 67 a power-law, but the exponent of the power-law (i.e., the negative slope
 68 of the curve) decreases with the increase of the minimum burned area
 69 s characterizing the class. However, all these distributions practically
 70 collapse into a single function F , as shown in Fig. 2(b) (again extracted
 71 from Corral et al. (2008)), through the simple scale transformation
 72 $\tau \rightarrow R(s)\tau$ and $D(\tau|s) \rightarrow D(\tau|s)/R(s)$, where $R(s)$ is the rate of fire
 73 occurrence in class s (defined as the mean number of fires per unit time
 74 with burned area greater than or equal to s). This interesting discovery,
 75 formally revealed by the relationship

$$D(\tau|s) = R(s)F(R(s)\tau) \quad (1)$$

76 allows one to conclude that forest fires fulfill a scaling law for the time in-
 77 tervals separating successive fires without necessarily displaying power-
 78 law distributions of the burned areas.

79 [Figure 2 about here.]

80 **Theoretical investigations on forest fire characteristics**

81 The attempts of deriving fire characteristics from purely theoretical
 82 arguments have been performed through two different classes of models.
 83 The models of the first class, known as self-organized critical forest-fire
 84 (SOCFF) models, are probabilistic cellular automata defined over a
 85 square lattice with L^2 sites. In the first version (Bak et al. (1990))
 86 each site is at each time step in one of three possible states: green

87 (i.e., not burning) tree; red (i.e., burning) tree; absence of vegetation.
88 The transition rules are very simple: (i) green trees become red if they
89 are close to red trees and remain green otherwise; (ii) red trees die
90 thus leaving the site empty; (iii) each empty site has a probability p of
91 becoming occupied by a green tree. Bak et al. (1990) state that their
92 model is a self-organized critical model capable of showing how the solar
93 energy absorbed continuously at low rate by vegetation can be randomly
94 dissipated through rare and disruptive events (the fires). However, the
95 agreement with real forests is, even qualitatively, rather poor because
96 the model generated fires are always present (in the form of travelling
97 fronts burning pieces of the boundaries of vegetational clusters).

98 The model proposed by Bak et al. (1990) is immediately criticized
99 by Drossel and Schwabl (1992) who point out some of its critical aspects
100 and introduce a second parameter (f), called "lightning parameter" by
101 means of which they modify rule (i) saying that green trees not close to
102 red ones have a probability f to become red. This variation introduces
103 a random exogenous mechanism of fire ignition and is essential for cre-
104 ating clusters of fires with areas distributed as power-laws. A number
105 of variants of the SOCGF model are immediately proposed by various
106 authors (see Clar et al. (1996) for a review). In particular, Drossel and
107 Schwabl (1993) introduce a third parameter, called "tree immunity" in
108 order to modify, once more, rule (i) by saying that green trees have a
109 certain probability of remaining such when they are close to red trees.
110 Later (Song et al. (2001)) this variant is shown to give rise to distribu-
111 tions of burned areas that can be approximated with two power-laws,
112 one for small-medium fires and one for large fires. A similar result is
113 obtained by Schenk et al. (2000) by stressing the finite-size effects in
114 SOCGF models.

115 In the second class of models, here called two-layer models, the
116 forest is described by two sets of ordinary differential equations, one
117 associated with the lower layer composed of bryophytes, herbs, shrubs
118 or any mix of these plants and the other associated with the upper layer
119 composed of plants and trees of various species. The growth of the two
120 layers in the absence of fire is described in the standard continuous time

121 form

$$\begin{aligned}\dot{L} &= r_L L \left(1 - \frac{L}{K_L}\right) - \alpha LU \\ \dot{U} &= r_U U \left(1 - \frac{U}{K_U}\right)\end{aligned}\tag{2}$$

122 where r and K indicate growth rate and carrying capacity and αLU
123 is the surplus of mortality in the lower layer due to light interception
124 caused by tree canopy. Thus, in the absence of fire, trees grow logisti-
125 cally toward the carrying capacity K_U , while plants of the lower layer
126 tend toward $(1 - \alpha K_U/r_L)K_L$. The validity and limitations of eq. (2)
127 are discussed in Casagrandi and Rinaldi (1999), where realistic values of
128 the five vegetational parameters ($r_L, r_U, K_L, K_U, \alpha$) are also suggested.

129 As for the fire, there are two options. The first (Casagrandi and
130 Rinaldi (1999)) is to add two extra-variables representing the burning
131 (red) biomasses in the two layers and describe the propagation of the
132 fire to the green biomasses L and U through suitable fire attack rates.
133 This gives a model with four ordinary differential equations which is,
134 however, a so-called slow-fast model because the green biomasses grow
135 very slowly (typically over years), while the red ones become suddenly
136 very high when the fire starts and then practically drop to zero after a
137 very short time (typically a few days or weeks).

138 The second option (Maggi and Rinaldi (2006)) is to push the slow-
139 fast nature of the system to the extreme, by considering fires as devas-
140 tating events capable of reducing instantaneously the green biomasses
141 of finite amounts. This can be accomplished, without adding extra
142 differential equations, by defining as shown in Fig. 3(a) the pre- and
143 post-fire manifolds \mathcal{X}^- and \mathcal{X}^+ and the map from \mathcal{X}^- to \mathcal{X}^+ interpreting
144 the impact of the fire.

145 [Figure 3 about here.]

146 The pre-fire manifold \mathcal{X}^- in Fig. 3(a) is piece-wise linear and non-
147 increasing, and the set below the manifold is convex. The first property
148 is obvious because less fuel originated from trees (i.e. less trees) is nec-
149 essary for fire ignition if more fuel originated from bushes is available
150 on the ground. The second property simply says that if $x' = (B', T')$
151 and $x'' = (B'', T'')$ are two states of the forest at which fire ignition is

152 not possible (i.e. two points below the manifold \mathcal{X}^-) no mix of these
 153 two states (i.e. no points of the segment connecting x' with x'') can
 154 give rise to fire ignition. A formal support of these two properties can
 155 be found in Maggi and Rinaldi (2006). The geometry of the pre-fire
 156 manifold allows one to sharply identify surface fires (vertical segment
 157 of \mathcal{X}^-), crown fires (horizontal segment of \mathcal{X}^-) and mixed fires (oblique
 158 segment of \mathcal{X}^-). By definition, surface fires do not involve the up-
 159 per layer, so that the post-fire conditions are on the vertical segment
 160 characterized by $L^+ = \lambda_L \rho_L K_L = \lambda_L L^-$. In other words, ρ_L is, by
 161 definition, the portion of the lower layer carrying capacity K_L at which
 162 surface fires occur and λ_L is the portion of the lower layer biomass that
 163 survives to surface fire. Similarly, fires in the upper layer are char-
 164 acterized by a vertical instantaneous transition from $U^- = \rho_U K_U$ to
 165 $U^+ = \lambda_U U^-$. The most extreme surface fire is represented by the tran-
 166 sition $S^- \rightarrow S^+$, while the most extreme crown fire is represented by
 167 the transition $C^- \rightarrow C^+$. The assumption that mixed fires initiate on
 168 the segment $C^- S^-$ implies, by continuity, that post-fire conditions are
 169 on a curve connecting C^+ and S^+ which, for simplicity, is identified
 170 with the linear segment $C^+ S^+$.

171 Fire sequences can be easily obtained from the model, as shown in
 172 Fig. 3(b). Starting from a given initial condition, say point 0, one
 173 numerically integrates the differential eqs. (2) until the solution hits
 174 the pre-fire manifold \mathcal{X}^- at point 1^- . Then, using the map $\mathcal{X}^- \rightarrow \mathcal{X}^+$
 175 one can determine the post-fire conditions, namely point 1^+ . Finally,
 176 the procedure is iterated and a series of fires ($2^- \rightarrow 2^+$), ($3^- \rightarrow 3^+$), ...
 177 is obtained.

178 A detailed analysis of this minimal model (Maggi and Rinaldi (2006))
 179 has shown that it is very flexible and can reproduce, by tuning its
 180 parameters, the fire regimes of savannas, boreal forests and Mediter-
 181 ranean forests. The dependence of the model behavior upon its nu-
 182 merous parameters has been thoroughly investigated in Dercole and
 183 Maggi (2005) and in Bizzarri et al. (2008). Moreover, long series of
 184 model generated fires have been statistically analyzed and the result
 185 is that the distributions of the total biomasses burned by fire events
 186 (i.e., $L^- + U^- - L^+ - U^+$) can often be approximated by three power

187 laws (see Fig. 5 in Maggi and Rinaldi (2006)). This result is somehow
188 similar to that shown in Fig. 1(b), where, however, the fire intensities
189 are identified with burned areas.

190 It is worth noticing that in none of the above mentioned studies
191 the models have been validated against the data collected on a specific
192 forest site. This is perfectly in line with the aim of the studies, which
193 was to show that the models could produce fire regimes similar to those
194 qualitatively observed in various biomes of the world.

195 **Analysis of a spatially extended two-layer forest fire model**

196 The models reviewed in the previous section are definitely poor and
197 over-simplified from a biological point of view even if they support to a
198 certain extent some of the characteristics of forest fires emerging from
199 field data. SOCOFF models reduce the growth of vegetation to a sort
200 of unrealistic ballet of trees born in empty sites and then burned by
201 lightning, without giving any role to important physical factors such
202 as quantity of dead biomass on the ground or age of the plants which
203 are known to control the ignition of a fire and its propagation (Vie-
204 gas (1998)). By contrast, two-layer models are simply inappropriate
205 for describing properties concerning burned areas because they do not
206 explicitly contain space.

207 We therefore focus on a promising mix of the above models by spa-
208 tially extending on a square lattice with L^2 sites, the two-layer forest-
209 fire model. Thus, eq. (2) holds at each site, characterized however by
210 a different standing state (L, U) , and when the biomasses in one site
211 reach the pre-fire manifold \mathcal{X}^- , a fire is ignited in that site of the for-
212 est and the biomasses of that site are reduced in accordance with the
213 map described in Fig. 3(a). Moreover, the fire propagates to neigh-
214 boring sites provided the vegetation in those sites is almost ready to
215 burn, i.e. provided the biomasses (L, U) are ε -close to the pre-fire man-
216 ifold \mathcal{X}^- . In order to simplify the dynamics we assume, in accordance
217 with Drossel and Schwabl (1992), that the propagation is a sort of in-
218 stantaneous avalanche, since the time in which a forest cluster burns
219 down is much shorter than the time in which a tree grows. This means
220 that when the pre-fire manifold is reached at one site, the fire instan-

221 taneously propagates to an entire forest cluster delimited by sites in
222 which the biomasses (L, U) are at least ε -far from the pre-fire manifold
223 \mathcal{X}^- . Thus, the area burned by fire can be measured by the number of
224 sites in the cluster.

225 Long simulations of the model allow one to generate long time se-
226 ries of fires with associated burned areas and times of occurrence. Since
227 simulations involve time-discretization, it can happen (very rarely how-
228 ever) that two fires occur at the same time. In these cases one of the
229 two fires is simply delayed of one time step.

230 In order to avoid finite-size effects we have been forced to work with
231 large lattices and this is why, in order to keep computational effort un-
232 der control, we have selected the model described in Maggi and Rinaldi
233 (2006) which involves $2L^2$ differential equations, i.e. one half of those
234 that would be required by the model proposed in Casagrandi and Ri-
235 naldi (1999). Simulations must be very long because transients toward
236 attractors of the extended forest model can be extremely long, in par-
237 ticular when the local dynamics, i.e. the dynamics of a single isolated
238 site, are chaotic (see Fig. 4 which shows that a reliable estimate of the
239 mean and standard deviation of the burned areas is obtained only after
240 three hundred thousand years!).

241 [Figure 4 about here.]

242 Despite these computational difficulties, we have been able to per-
243 form reliable statistics of the burned areas and of the time of occurrence
244 of the fires for different values of the parameters of the model. In par-
245 ticular, we have varied the parameter ε that controls the tendency of
246 the fire to penetrate into parts of the forest which are not yet ready to
247 burn. Obviously, this parameter depends upon the dominant species
248 present and can therefore vary remarkably in particular at continental
249 scale. Higher values of ε indicate lower resistance to fire propagation,
250 i.e. lower tree immunity, as defined in Drossel and Schwabl (1993), Al-
251 bano (1995) and Song et al. (2001) in their studies on SOCFF models.
252 Higher values of ε should therefore facilitate the occurrence of larger
253 fires and this is, indeed, what we have systematically found with our
254 simulations, as shown in Fig. 5 obtained for parameter values in the
255 range suggested in Maggi and Rinaldi (2006) for Mediterranean forests.

257 Figure 5 shows that the three basic types of distributions identified
 258 through empirical studies (see Fig. 1) can be produced by our model by
 259 varying the control parameter ε . Another interesting property of our
 260 model is that large fires, which are associated with the steepest slopes
 261 of the distributions of the burned areas, are mixed fires, while a relevant
 262 percentage of the small fires are surface fires. In other words, the results
 263 suggest that the existence of different slopes in the distributions of the
 264 burned areas might be due to the existence of differently structured
 265 fires. This has also been suggested in Schenk et al. (2000) but with
 266 totally different and less biologically based arguments.

267 Finally, long series of model generated fires have allowed us to esti-
 268 mate the probability density $D(\tau|s)$ of the time intervals τ separating
 269 successive fires with burned areas greater than or equal to s . A typical
 270 result of this analysis is shown in Fig. 6(a) which compares favourably
 271 with Fig. 2(a).

273 This means that our model captures also the processes that control the
 274 times of occurrence of the fires and not only the mechanism regulating
 275 the severity of the fires, i.e. the burned areas. But the qualitative
 276 agreement of our model with the empirical evidence goes even further.
 277 In fact, the similarity of Fig. 2(b) with Fig. 6(b), obtained through
 278 simulation, proves that the model is endowed with the scaling law (1)
 279 discovered on purely empirical grounds (Corral et al. (2008)).

280 **Concluding remarks**

281 We have shown that all statistical properties of forest fires discovered
 282 in the last decade through the analysis of available data can be derived
 283 from a biological based model in which the three phases of vegetational
 284 growth, fire ignition and fire propagation are clearly identified. In such
 285 a model the forest extends over a square lattice of L^2 sites and is com-
 286 posed of a lower and an upper layer. The two layers grow logistically,
 287 but the upper one reduces the light available to the lower one, thus
 288 damaging its growth. Fires are devastating instantaneous events that

289 occur only when the mix of biomasses of the two layers reach partic-
290 ular values. The rationale for this assumption is as follows. We know
291 (see, for example, Viegas (1998)) that fire ignition in a forest is possible
292 only if dead biomass on the ground is above a certain threshold, but
293 since the biochemical processes regulating the mineralization of dead
294 biomass are relatively fast with respect to plant growth (Esser et al.
295 (1982); Seastedt (1988)) it can be reasonably assumed that the rate
296 of mineralization (proportional to the amount of dead biomass) equals
297 the inflow rate of new necromass, which, in turn, is proportional to the
298 standing biomass in the two layers. Thus, in conclusion, the biomasses
299 of the two layers are appropriate indicators of fuel on the ground, so
300 that fire ignition is possible only at sites where the standing biomasses
301 reach specific conditions (called pre-fire conditions). When the fire is
302 ignited at one site, it immediately propagates to the neighbouring sites
303 if these are ε -close to their pre-fire conditions and this process is re-
304 peated in an avalanche like manner and stops only when the burning
305 cluster is delimited by sites which are ε -far to their pre-fire conditions.

306 The combination of these slow and fast processes determines the
307 behavior of the whole forest model which for parameter values in the
308 ranges suggested in Maggi and Rinaldi (2006) for Mediterranean forests
309 turns out to be chaotic. In other words, the slow and continuous growth
310 of the two vegetational layers is punctuated by fires which occur in an
311 apparently random way in space and time and has statistical properties
312 consistent with those discovered empirically.

313 It is important to remark that the model proposed in this paper is
314 nothing but the extension to a network of sites of the minimal model
315 proposed in Maggi and Rinaldi (2006) for a single site. In other words,
316 the model is still a minimal model that, as such, can not be calibrated
317 for performing real time fire predictions in any specific forest, but rather
318 be used to characterize and classify the fire regimes of large classes of
319 forests.

320 It is also interesting to remark that the model is fully determin-
321 istic and spatially homogeneous, so that the emergence of the above
322 statistical properties does not seem to be necessarily related with the
323 randomness of meteorological conditions (soil moisture, wind speed, ...)

324 or with geophysical heterogeneity. However, in accordance with Bessie
325 and Johnson (1995) and Minnich and Chou (1997), we firmly believe
326 that meteorological randomness and geophysical heterogeneity should
327 amplify the chaoticity generated by the deterministic mechanisms of
328 growth, ignition and propagation we have considered. Checking if this
329 is true could be an interesting point for further investigation, in partic-
330 ular for assessing the impact of environmental change on fire regimes.
331 But certainly more interesting would be to try to explain with the model
332 important regional characteristics of fire regimes that have been discov-
333 ered from data. For example, the east to west gradient of the slopes of
334 the power-law distribution across US (Malamud et al. (2005)), might
335 be a consequence of a similar gradient in some of the parameters of the
336 model, that control the slopes of the distributions.

337 **References**

- 338 Albano, E. V., 1995. Spreading analysis and finite-size scaling study of
339 the critical behavior of a forest fire model with immune trees. *Physica*
340 *A* 216, 213–226.
- 341 Bak, P., Chen, K., Tang, C., 1990. A forest-fire model and some
342 thoughts on turbulence. *Phys. Lett. A* 147, 297–300.
- 343 Bessie, W. C., Johnson, E. A., 1995. The relative importance of fuels
344 and weather on fire behavior in subalpine forests. *Ecology* 76 (3),
345 747–762.
- 346 Bizzarri, F., Storace, M., Colombo, A., 2008. Bifurcation analysis of an
347 impact model for forest fire prediction. *Int. J. Bifurcat. Chaos* 18 (8),
348 2275–2288.
- 349 Casagrandi, R., Rinaldi, S., 1999. A Minimal Model for Forest Fire
350 Regimes. *Am. Nat.* 153 (5), 527–539.
- 351 Clar, S., Drossel, B., Schwabl, F., 1996. Forest fires and other examples
352 of self-organized criticality. *J. Phys. Condens. Matter* 8 (37), 6803–
353 6824.
- 354 Corral, A., Telesca, L., Lasaponara, R., 2008. Scaling and correlations

355 in the dynamics of forest-fire occurrence. *Phys. Rev. E* 77, 016101(1–
356 7).

357 Dercole, F., Maggi, S., 2005. Detection and continuation of a border
358 collision bifurcation in a forest fire model. *Appl. Math. Comput.* 168,
359 623–635.

360 Drossel, B., Schwabl, F., 1992. Self-organized critical forest-fire model.
361 *Phys. Rev. Lett.* 69 (11), 1629–1632.

362 Drossel, B., Schwabl, F., 1993. Forest-fire model with immune trees.
363 *Physica A* 199 (2), 183–197.

364 Esser, G., Aselmann, I., Lieth, H., 1982. Modelling the Carbon Reser-
365 voir in the System Compartment "Litter". *Mitt. Geol.-Paläont. Inst.*
366 Univ. Hamburg 52, 39–58.

367 Lasaponara, R., Santulli, A., Telesca, L., 2005. Time-clustering analysis
368 of forest-fire sequences in southern Italy. *Chaos Soliton. Fract.* 24,
369 139–149.

370 Maggi, S., Rinaldi, S., 2006. A second-order impact model for forest
371 fire regimes. *Theor. Popul. Biol.* 70, 174–182.

372 Malamud, B. D., Millington, J. D. A., Perry, G. L. W., 2005. Charac-
373 terizing wildfire regimes in the United States. *Proc. Nat. Acad. Sci.*
374 U.S.A. 102 (13), 4694–4699.

375 Malamud, B. D., Morein, G., Turcotte, D. L., 1998. Forest Fires: An
376 Example of Self-Organized Critical Behavior. *Science* 281, 1840–1841.

377 Minnich, R. A., Chou, Y. H., 1997. Wildland Fire Patch Dynamics in
378 the Chaparral of Southern California and Northern Baja California.
379 *Int. J. Wildland Fire* 7 (3), 221–248.

380 Reed, W. J., McKelvey, K. S., 2002. Power-law behaviour and paramet-
381 ric models for the size-distribution of forest fires. *Ecol. Model.* 150,
382 239–254.

383 Ricotta, C., 2003. Fractal size distributions of wildfires in hierarchical
384 landscapes: *Natura facit saltus?* *Comm. Theor. Biol.* 8, 93–101.

- 385 Ricotta, C., Arianoutsou, M., Díaz-Delgado, R., Duguy, B., Lloret, F.,
386 Maroudi, E., Mazzoleni, S., Moreno, J. M., Rambal, S., Vallejo, R.,
387 Vázquez, A., 2001. Self-organized criticality of wildfires ecologically
388 revisited. *Ecol. Model.* 141, 307–311.
- 389 Ricotta, C., Avena, G., Marchetti, M., 1999. The flaming sandpile:
390 self-organized criticality and wildfires. *Ecol. Model.* 119, 73–77.
- 391 Ricotta, C., Micozzi, L., Bellelli, M., Mazzoleni, S., 2006. Characteriz-
392 ing self-similar temporal clustering of wildfires in the Cilento National
393 Park (Southern Italy). *Ecol. Model.* 197, 512–515.
- 394 Schenk, K., Drossel, B., Schwabl, F., 2000. Finite-size effects in the self-
395 organized critical forest-fire model. *Eur. Phys. J. B* 15 (1), 177–185.
- 396 Seastedt, T., 1988. Mass, Nitrogen, and Phosphorus Dynamics in Fo-
397 liage and Root Detritus of Tallgrass Prairie. *Ecology* 69 (1), 59–65.
- 398 Song, W., Fan, W., Wang, B., Zhou, J., 2001. Self-organized criticality
399 of forest fire in China. *Ecol. Model.* 145, 61–68.
- 400 Telesca, L., Amatulli, G., Lasaponara, R., Lovallo, M., Santulli, A.,
401 2005. Time-scaling properties in forest-fire sequences observed in
402 Gargano area (southern Italy). *Ecol. Model.* 185, 531–544.
- 403 Viegas, D. X., 1998. Forest Fire Propagation. *Phil. Trans. R. Soc. Lond.*
404 A 356 (1748), 2907–2928.

406	1	Three examples of cumulative distributions of burned areas	
407		obtained from data: (a) Clearwater National Forest (US) re-	
408		drawn from Reed and McKelvey (2002); (b) Gargano (Italy)	
409		redrawn from Telesca et al. (2005); (c) Venaco (Corse, France)	
410		redrawn from Ricotta et al. (2001). The distribution in (a)	
411		cannot be approximated with a power law, while the distri-	
412		butions in (b) and (c) are approximated with three and two	
413		power laws, respectively.	15
414	2	Results of the analysis of the time intervals τ separating suc-	
415		cessive fires in Italy (redrawn from Corral et al. (2008)). (a)	
416		Probability densities $D(\tau s)$ for different minimum burned ar-	
417		reas s . (b) The previous densities after rescaling by the mean	
418		fire rate $R(s)$ (notice that the rescaling yields dimensionless	
419		axes).	16
420	3	Two-layer model behavior. (a) The pre- and post-fire mani-	
421		folds \mathcal{X}^- and \mathcal{X}^+ ; the dotted lines with double arrows are in-	
422		stantaneous transitions from \mathcal{X}^- to \mathcal{X}^+ due to a fire; horizon-	
423		tal (vertical) lines correspond to surface (crown) fires; oblique	
424		lines starting from the segment C^-S^- of \mathcal{X}^- correspond to	
425		mixed fires. (b) State portrait of the model; continuous lines	
426		with a single arrow represent the growing phase of the forest	
427		and are described by eq. (2).	17
428	4	Estimate $\hat{\mu}$ and $\hat{\sigma}$ of the mean and standard deviation of the	
429		burned areas as a function of the observation time for the	
430		model with $\varepsilon = 0.08, r_L = 3/8, r_U = 1/16, K_L = K_U =$	
431		$1, \alpha = 129/800, \rho_L = 0.85, \rho_U = 14/15, \sigma_L = 0.6, \sigma_U =$	
432		$0.35, \lambda_L = \lambda_U = 10^{-4}$	18
433	5	Three examples of cumulative distributions $P(s) = \text{prob}[\text{burned area} \geq$	
434		$s]$ obtained from the model for different parameter values:	
435		(a): $\varepsilon = 0.06$; (b): $\varepsilon = 0.07$; (c): $\varepsilon = 0.08$. Other parameter	
436		values as specified in the caption of Fig. 4.	19
437	6	Results of the analysis of the time intervals τ separating suc-	
438		cessive fires generated by the model with parameter values	
439		as specified in the caption of Fig. 4. (a) Probability densi-	
440		ties $D(\tau s)$ for minimum burned areas s . (b) The previous	
441		densities after rescaling by the mean fire rate $R(s)$	20

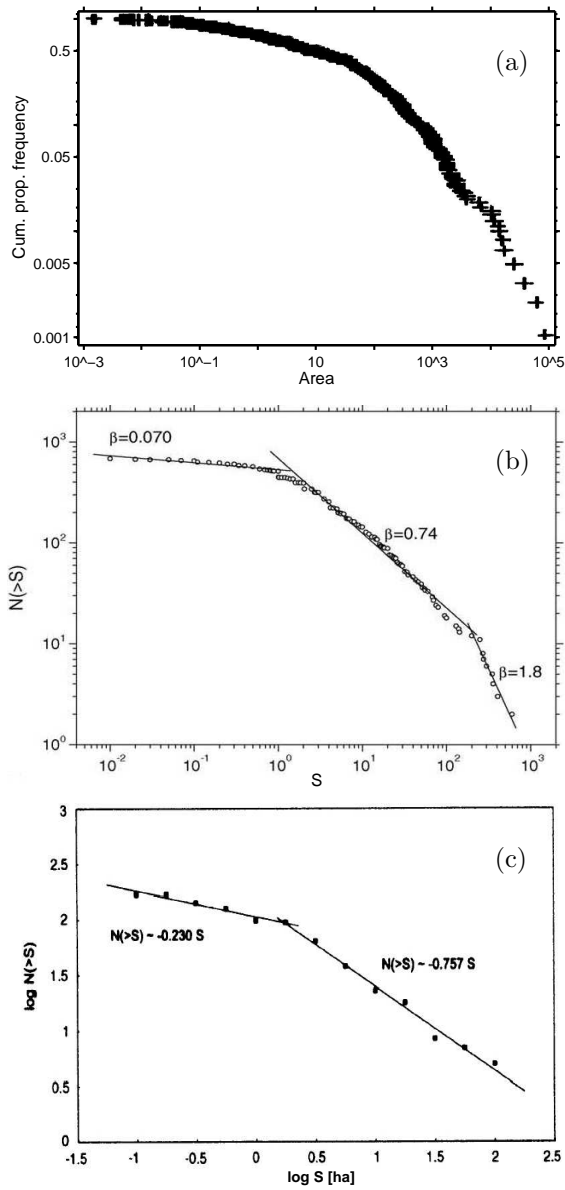


Figure 1: Three examples of cumulative distributions of burned areas obtained from data: (a) Clearwater National Forest (US) redrawn from Reed and McKelvey (2002); (b) Gargano (Italy) redrawn from Telesca et al. (2005); (c) Venaco (Corse, France) redrawn from Ricotta et al. (2001). The distribution in (a) cannot be approximated with a power law, while the distributions in (b) and (c) are approximated with three and two power laws, respectively.

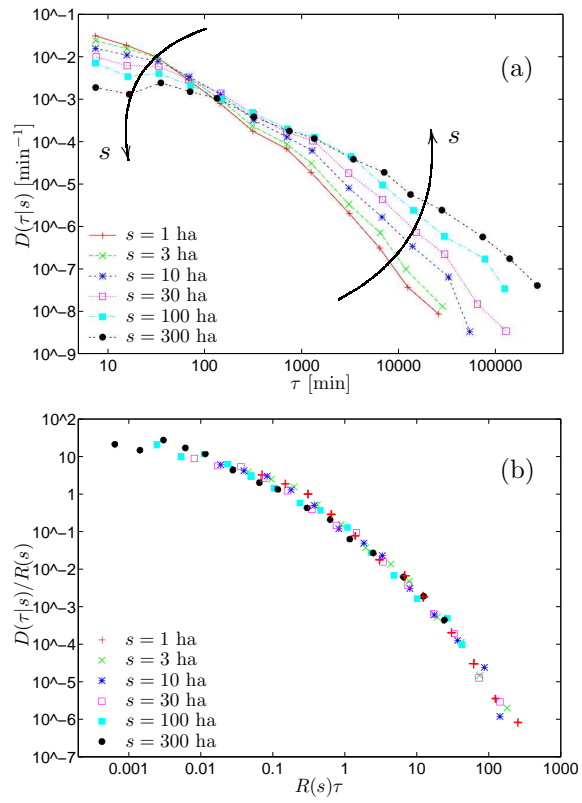


Figure 2: Results of the analysis of the time intervals τ separating successive fires in Italy (redrawn from Corral et al. (2008)). (a) Probability densities $D(\tau|s)$ for different burned areas s . (b) The previous densities after rescaling by the mean fire rate $R(s)$ (notice that the rescaling yields dimensionless axes).

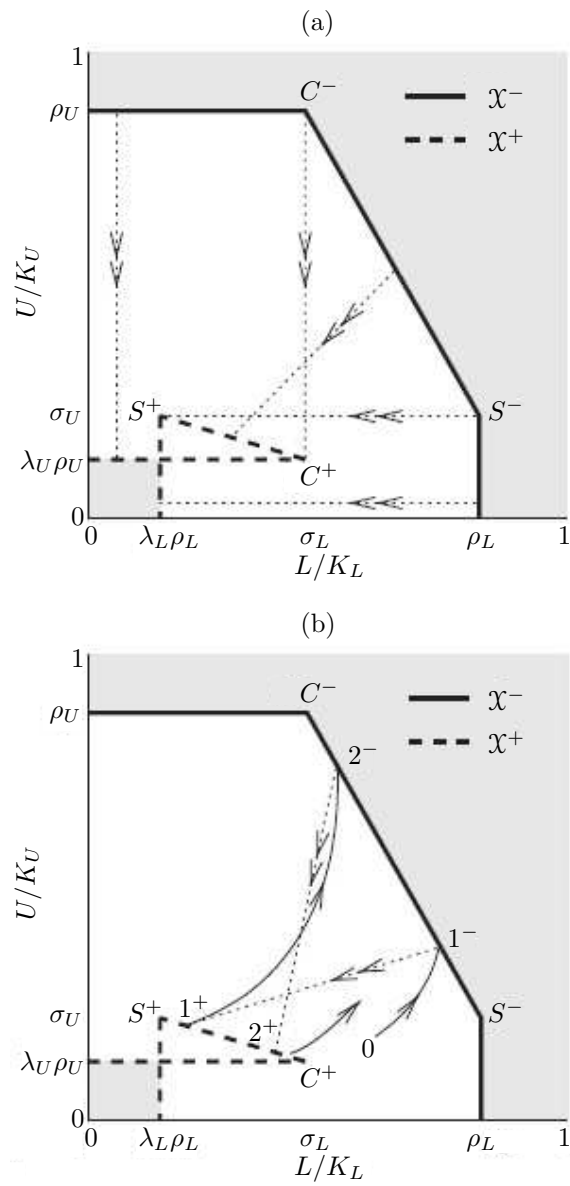


Figure 3: Two-layer model behavior. (a) The pre- and post-fire manifolds \mathcal{X}^- and \mathcal{X}^+ ; the dotted lines with double arrows are instantaneous transitions from \mathcal{X}^- to \mathcal{X}^+ due to a fire; horizontal (vertical) lines correspond to surface (crown) fires; oblique lines starting from the segment C^-S^- of \mathcal{X}^- correspond to mixed fires. (b) State portrait of the model; continuous lines with a single arrow represent the growing phase of the forest and are described by eq. (2).

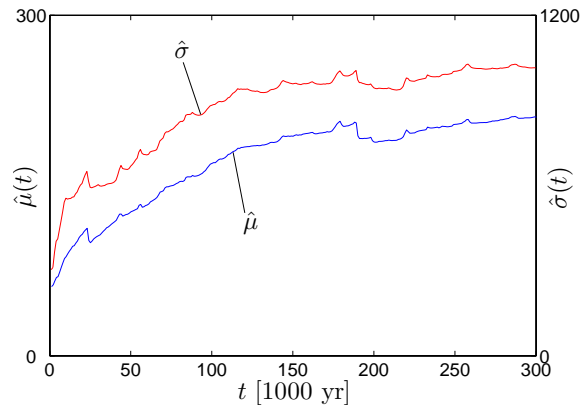


Figure 4: Estimate $\hat{\mu}$ and $\hat{\sigma}$ of the mean and standard deviation of the burned areas as a function of the observation time for the model with $\varepsilon = 0.08$, $r_L = 3/8$, $r_U = 1/16$, $K_L = K_U = 1$, $\alpha = 129/800$, $\rho_L = 0.85$, $\rho_U = 14/15$, $\sigma_L = 0.6$, $\sigma_U = 0.35$, $\lambda_L = \lambda_U = 10^{-4}$.

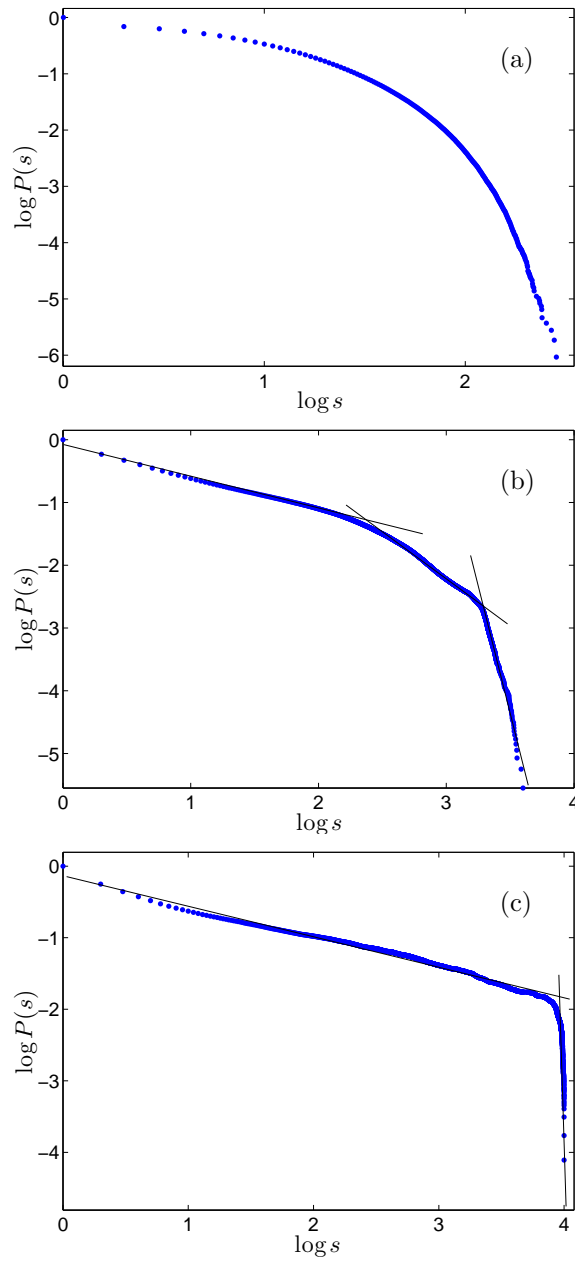


Figure 5: Three examples of cumulative distributions $P(s) = \text{prob}[\text{burned area} \geq s]$ obtained from the model for different parameter values: (a): $\varepsilon = 0.06$; (b): $\varepsilon = 0.07$; (c): $\varepsilon = 0.08$. Other parameter values as specified in the caption of Fig. 4.

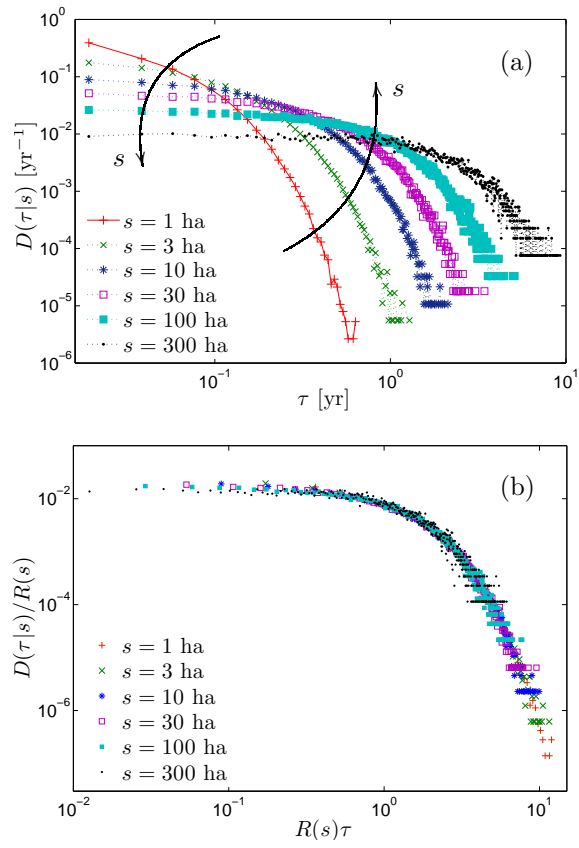


Figure 6: Results of the analysis of the time intervals τ separating successive fires generated by the model with parameter values as specified in the caption of Fig. 4. (a) Probability densities $D(\tau|s)$ for minimum burned areas s . (b) The previous densities after rescaling by the mean fire rate $R(s)$.